Available online at www.sciencedirect.com

ScienceDirect

journal homepage: www.elsevier.com/locate/he

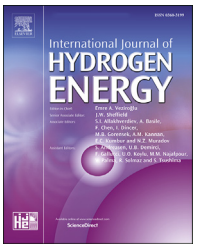

A solar and wind driven energy system for hydrogen and urea production with CO_2 capturing

Haris Ishaq[*], *Osamah Siddiqui, Ghassan Chehade, Ibrahim Dincer*

Clean Energy Research Laboratory, Faculty of Engineering and Applied Science, University of Ontario Institute of Technology, Ontario, Canada

HIGHLIGHTS

- A novel solar-wind hybrid energy system is developed for hydrogen and urea production.
- Produced hydrogen is converted into ammonia and synthesizes urea by capturing CO_2.
- The amount of electrical power produced by the system is 2.14 MW.
- Designed system produces 518.4 kmol/d of H_2 and synthesizes 86.4 kmol/d of urea.

ARTICLE INFO

Article history:
Received 2 October 2019
Received in revised form
24 January 2020
Accepted 27 January 2020
Available online xxx

Keywords:
Solar energy
Wind power
Hydrogen
Urea synthesis
CO_2 capture
Efficiency

ABSTRACT

A novel solar PV and wind energy based system is proposed in this study for capturing carbon dioxide as well as producing hydrogen, urea and power. Both Aspen Plus and EES software packages are employed for analyses and simulations. The present system is designed in a way that PEM electrolyzer is powered by the wind turbines for hydrogen production, which is further converted into ammonia and then synthesizes urea by capturing CO_2 and additional power is supplied to the community. The solar PV is employed to power the cryogenic air separation unit and the additional power is used for the industrial purpose. In the proposed system, ammonia does not only capture CO_2 but also synthesizes urea for fertilizer industry. The amount of electrical power produced by the system is 2.14 MW. The designed system produces 518.4 kmol/d of hydrogen and synthesizes 86.4 kmol/d of urea. Furthermore, several parametric studies are employed to investigate the system performance.

© 2020 Hydrogen Energy Publications LLC. Published by Elsevier Ltd. All rights reserved.

Introduction

In recent decades, industrialization has caused a massive environmental burden owing to the colossal amounts of detrimental emissions. According to a report, 7.0 Gt of CO_2 emissions were recorded in the American region [1]. Hence, numerous efforts to mitigate these harmful emissions are being conducted across the globe. One such methodology includes CO_2 capture. There are various methods for CO_2 capture in the literature using monoethanolamine (MEA) and ammonia that have already been investigated [2]. However, promising options entail the capture of CO_2 and subsequent production of useful commodities. Capturing anthropogenic or industrial flue gas CO_2 and producing urea is one such option that enables the capturing of an environmentally harmful substance to produce one of the most important components in fertilizer production. The urea is considered as the backbone of any fertilizer industry and ammonia synthesis from

* *Corresponding author.*
E-mail address: haris.ishaq@uoit.net (H. Ishaq).
https://doi.org/10.1016/j.ijhydene.2020.01.208
0360-3199/© 2020 Hydrogen Energy Publications LLC. Published by Elsevier Ltd. All rights reserved.

Please cite this article as: Ishaq H et al., A solar and wind driven energy system for hydrogen and urea production with CO_2 capturing, International Journal of Hydrogen Energy, https://doi.org/10.1016/j.ijhydene.2020.01.208

renewable hydrogen can be very promising for sustainable future. This paper presents the H_2 and urea synthesis using renewable energy sources.

Apak [3] studied the potential of using ammonia for mitigating the anthropogenic CO_2 emissions. In addition, he emphasized on the possibility of producing urea trough the reaction with ammonia as CO_2 is already utilized as a raw material for urea synthesis. Barzagli et al. [4] investigated CO_2 capture from flue gas through ammonia as well as amines to form carbamate. Further, the conversion of carbamate to urea was also studied experimentally. Furthermore, Barzagli et al. [5] studied the CO_2 capture through both aqueous and gaseous ammonia. The capture process was investigated at ambient conditions. They reported capturing amounts up to 99% according to the ammonia concentrations. Also, the production of urea from the formed ammonium carbamate was tested for the temperature range of 120°C–140 °C.

Bandyopadhyay [6] presented a research study on the comparison between ammonia and amine absorption to analyse the reduction in greenhouse gas emissions. McLaron and Duncan [7] presented a testing criteria of NH_3 based carbon capturing using multi-pollutant technology control and provided a comparison of existing CO_2 capturing plants and MEA based CO_2 capturing. Kozak [8] investigated the chilled ammonia process to capture carbon from flue gas in combined cycles from coal-fired boilers and natural gas cycles. The chilled ammonia process ingrates an absorption system, a flue gas cooling system and a regeneration system in a closed-loop. They reported 80% CO_2 capture efficiency below the design capture efficiency of 90%. Calvo et al. [9] performed a similar study for CO_2 capture by chilled ammonia solution and its application in cement plants. A rate-based model was developed and simulated in Aspen-Plus for cement plant-like flue gas composition to obtain efficiencies using energy and exergy methods. The results show a minimum exergy need of 0.92 MJ/kg CO_2 at 85% capture energy efficiency. Similarly, Rhee et al. [10] performed analysis for CO_2 capture by ammonia in the ironmaking industry by changing the operating conditions such of the absorption and regeneration temperature, flow-rate of ammonia solution and the stream ration for removing slipped ammonia. The results of changing the NH_3 concertation showed over 90% CO_2 removal efficiencies and the regeneration temperature of 5, 7, 9 wt% ammonia solution were 87, 83, and 78 °C respectively. Gaspar et al. [11] investigated and optimized a CO_2 capture system using aqueous ammonia as solvent in Aspen-Plus software. The proposed layout replaces the traditional solvent-based CO_2 stripper with a thermal decomposition reactor. The results showed 80% of CO_2 could be captured in a low heat thermal reactor which reduces significantly the energy penalty of the capture process.

Ciferno et al. [12] developed a study on the use of aqueous ammonia to capture CO_2 from flue gas. They pointed out the importance of the low cost of the chemical, the higher loading capacity, and the potential for production of ammonium sulfate as a by-product. The experimental study performed by Kozak et al. [8] on the chilled ammonia process showed high potential compared to the conventional amine-based process. Mainly, the thermal energy requirements for the regeneration of the ammonia is found to be much lower than the one found with Ethanolamine (MEA). Also, the total power output obtained for the chilled ammonia process is higher than MEA, Moreover, the efficiency assessment results, showed that the ammonia process is more efficient than the MEA process. Puxty et al. [13] developed a model to study the kinetic rate of absorption of CO_2 by aqueous ammonia and compared it with MEA by varying the concentrations and temperatures. Qin et al. [14] achieved to model the heat of absorption of CO_2 by aqueous ammonia and proposed that the results can be used to model CO_2–NH_3–H_2O system.

Dave et al. [15] developed an Aspen Plus model to simulate the aqueous ammonia-based process. They proposed to use an ammonia concentration of 5 wt% and absorption temperature of 10 °C to avoid precipitation of ammonium bicarbonate and to restrict the ammonia slip during the absorption. Also, they compared the performance of the process to that of MEA and found that both processes were equivalent. Valenti et al. [16] evaluated the mass, energy and entropy flow for the chilled ammonia process in a simple thermodynamic model that included an estimation of the heat and power consumption along with a cost analysis for the carbon capture. Their results were compared to the MEA-based processes. Due to the simplicity of their model the accuracy of the model was not sufficient. Jilvero et al. [17] simulated the chilled ammonia process using a previously developed model by Kurz et al. [18] to evaluate the heat and electricity requirements. They indicated that the temperature of the cooling water in the regenerated stream is critical when assessing the efficiency of the system.

Integration of renewable energy gained lots of attention in the subject of CO_2 capture. Bennett et al. [19] proposed carbon capture powered by solar energy. The CO_2 absorber utilized direct chemical action by use of a reversible photoacid to absorb CO_2. Irradiation of the CO_2 solution resulted in CO_2 capture and removal by light photons and heat. Li at al [20]. Performed a feasibility study on integrating solar energy into a power plant with amine-based chemical absorption for CO_2 capture. Solar thermal energy is used to supply the energy demand for the stripper reboiler in post-combustion power plants. The finding of the study showed solar energy has the potential to supply the energy demand of the stripper boiler. However, the performance of the integrated power plant is primarily affected by the climate conditions and the CO_2 recovery ratios. Zhao at al [21]. Proposed a hybrid power system that utilizes mid-temperature solar heat and coal-fired power plant for CO_2 capture. The system replaces the high-quality steam of the Rankine cycle to heat the feedwater by solar heat at 300 °C. They reported an annual solar field cost reduction of 10.8 $/ton- CO_2, compared to 25.8 $/ton-$CO_2$ in a system with solar heat for direct solvent regeneration. Ordorica-Garcia et al. [22] proposed three solar-fossil hybrid energy systems: Integrated Solar Combined Cycle (ISCC), Solar-assisted post-combustion capture (SAPCAP), and Solar gasification with CO_2 capture. They concluded that the ISCC is the most promising concepts and successfully proven in a large-scale, While the other two processes require more testing in a pilot-scale with relatively low effort.

However, studies on renewable energy based CO_2 capturing systems entailing the ammonia to form urea were not conducted. A new approach to eliminate the harmful carbon dioxide via capturing it into ammonia by synthesizing ammonia is used in this study. The whole system is based on the power produced by solar PV and wind sources. The PEM

Please cite this article as: Ishaq H et al., A solar and wind driven energy system for hydrogen and urea production with CO_2 capturing, International Journal of Hydrogen Energy, https://doi.org/10.1016/j.ijhydene.2020.01.208

electrolyzer is powered by wind turbines which further converts into ammonia and then, captured CO_2 by synthesizing urea. The objective of this system is to design a novel renewable energy based system with the capability of capturing CO_2 and converting it into urea and analyzing the system through energetic and exergetic approach.

System description

The developed solar and wind energy based integrated system for the production of hydrogen, power and urea through carbon capturing is depicted in Fig. 1. The solar photovoltaic (PV) technology is utilized that generates power in the presence of sunlight. The PV panels comprise of semi-conductor materials that are excited when sunlight strikes the surface and electrons are emitted as a result. This excitation and electron emission results in the generation of clean and environmentally benign electricity. The power generated by the solar PV array is divided into two parts. The first part is sent to the cryogenic air separation unit (CASU) and the second part is sent to be utilized by the industry. The CASU comprises of a nitrogen separation system that intakes air and separates the contained nitrogen through cryogenic operation. The Aspen Plus flowsheet including cryogenic air separation unit and urea synthesis system is displayed in Fig. 2 Furthermore, the wind turbines generate power that is also utilized for two useful purposes. Firstly, a portion of the generated electricity is provided for domestic usage. Secondly, a part of the electricity generated is passed to the proton exchange membrane (PEM) water electrolyser. The PEM electrolyser intakes water and electricity as inputs and dissociates the water molecules to produce hydrogen. The produced hydrogen gas along with the nitrogen gas coming from the CASU are both passed to the ammonia synthesis reactor (ASR).

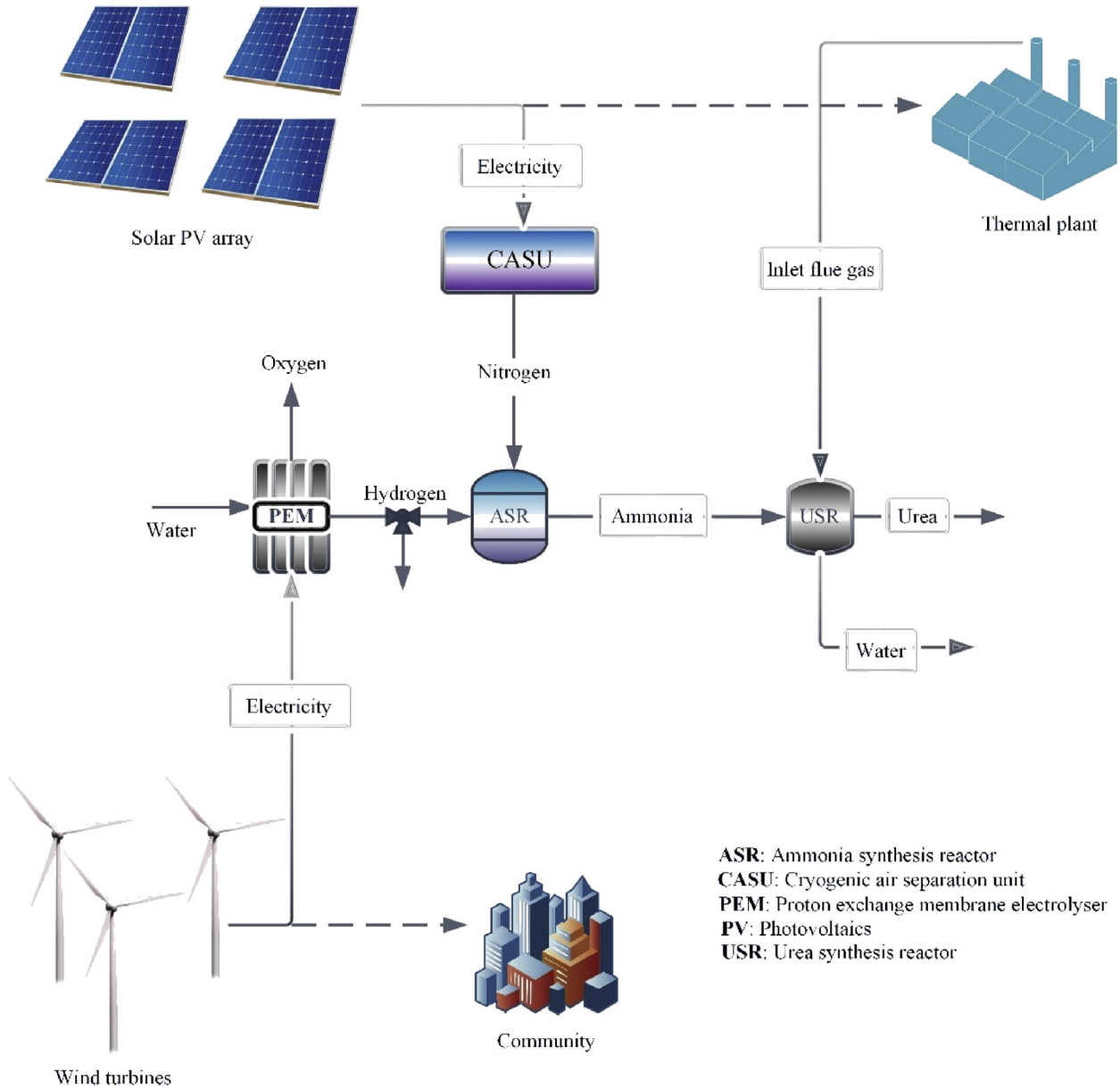

Fig. 1 – Schematic flowsheet of the proposed solar PV and wind driven system.

Please cite this article as: Ishaq H et al., A solar and wind driven energy system for hydrogen and urea production with CO_2 capturing, International Journal of Hydrogen Energy, https://doi.org/10.1016/j.ijhydene.2020.01.208

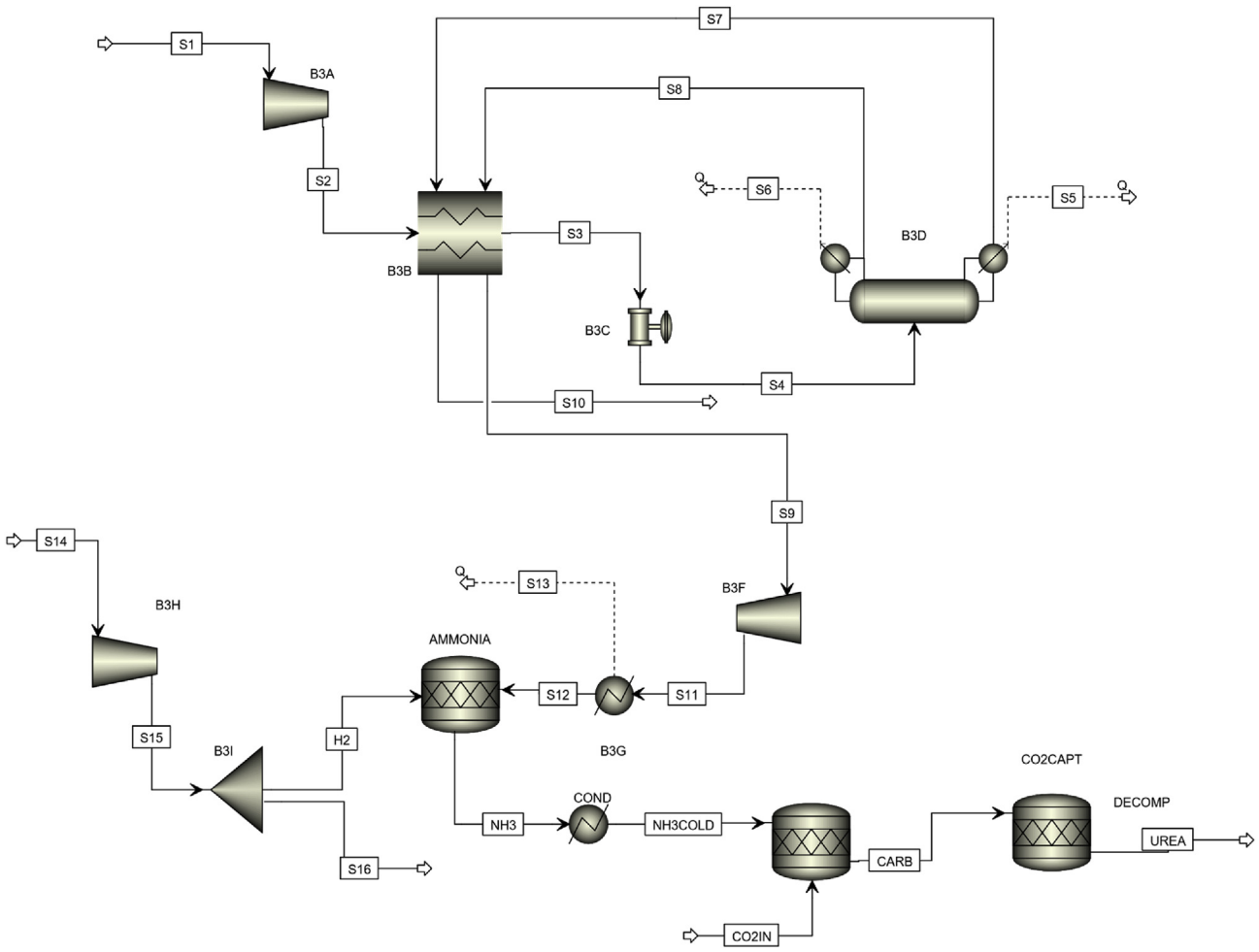

Fig. 2 – Aspen Plus flowsheet of the wind and solar PV based urea synthesis system.

In this subsystem, ammonia is synthesized and passed to the urea synthesis reactor (USR). The USR intakes ammonia along with the flue gas coming from the industry to capture the carbon dioxide contained in the flue gas and form a useful commodity of urea. Urea is utilized in various industries and applications across the globe. Especially, in the fertilizer industry urea plays a significant role. Hence, the developed system provides a novel way of capturing carbon dioxide and producing urea through environmentally benign energy resources of solar and wind energy. Along with urea as the useful output, the new system proposed also captures the carbon dioxide entailed in flue gases. The CO_2 removal efficiency is usually within the range of 50–80% [23] while this study assumes steady-state operation with fractional conversion of 1. Also, the system useful outputs include hydrogen as well as electrical power. Thus, trigeneration of hydrogen, urea and power is performed through renewable electricity and carbon capturing.

Analysis

A comprehensive thermodynamic analysis is conducted for the proposed system in order to examine the system performance. The software tools employed for the system modeling are Aspen Plus and EES. The energy and exergy analysis is also conducted for each individual system component and exergy destruction rate are also calculated. As exergy is the measure of useful work potential and exergy analysis also provides us with the exergy destruction rate within a system. This approach also provides us with an opportunity to improve the system performance by eliminating the exergy destructions, irreversibilities and heat losses. The following section describes the design equations for each subsystem and performance indicator for the overall system.

Solar photovoltaic array

The solar PV array takes solar radiation as the energy input and provides electrical output. The PV cells entail I–V characteristics that determine the maximum amount of power that can be extracted from the cell at a given solar radiation intensity. The power output from the PV cell is evaluated as

Table 1 – Design and operating parameters of the solar PV module.

Parameter	Value
Fill factor (*FF*)	0.5
Open circuit voltage (V_{OC})	0.6 V
Short circuit current (I_{SC})	3.0 A
Number of cells	1.1×10^6

Please cite this article as: Ishaq H et al., A solar and wind driven energy system for hydrogen and urea production with CO_2 capturing, International Journal of Hydrogen Energy, https://doi.org/10.1016/j.ijhydene.2020.01.208

$$\dot{P}_{PV} = FFV_{OC}I_{SC} \quad (1)$$

where FF denotes the fill factor that represents the ratio between the maximum PV power output and the product of the open-circuit voltage (V_{OC}) and the short-circuit current (I_{SC}):

$$FF = \frac{V_m I_m}{V_{OC} I_{SC}} \quad (2)$$

The total power output obtained from the PV array depends on the total number of cells utilized:

$$\dot{P}_{PV,tot} = FFV_{OC}I_{SC}N_{cells} \quad (3)$$

The parameters utilized for the analyses of the PV module are summarized in Table 1.

Further, the energy efficiency of the PV array can be determined as

$$\eta_{en} = \frac{\dot{P}_{PV,tot}}{\dot{Q}_{solar}} \quad (4)$$

where the solar input is denoted by $\dot{Q}_{solar}$. Also, the exergy efficiency is evaluated as

$$\eta_{en} = \frac{\dot{P}_{PV,tot}}{\dot{Q}_{solar}\left(1 - \frac{T_0}{T_{sun}}\right)} \quad (5)$$

Wind turbine

The power generated by the wind turbine is directly supplied to the PEM electrolyser and community considering average wind speed and correlation used to calculate this power is as follows:

$$P_{wt} = \frac{1}{2}\eta_{wt}A_{wt}\rho_{air}V^3C_{p,wt} \quad (6)$$

Proton exchange membrane electrolyser

The PEM electrolyser entails an input of electricity and water providing the outputs of hydrogen and oxygen. This dissociation of water molecules can be depicted by the following equation:

$$H_2O + \dot{P}_{in} \rightarrow H_2 + \frac{1}{2}O_2 \quad (7)$$

The change in Gibbs energy, as well as the change in entropy from the above reaction, can be used to denote the total required energy

$$\Delta H = T\Delta S + \Delta G \quad (8)$$

where H represents the enthalpy, T denotes the temperature in kelvin, G is the Gibbs energy and S is the entropy.

Furthermore, the hydrogen production rate via water electrolysis is evaluated as:

$$\dot{N}_{H_2} = \frac{IA}{2F} \quad (9)$$

where $\dot{N}_{H_2}$ represents the molar rate of hydrogen production, the current density is represented by I and F is the Faraday's constant.

Also, the current density and the cell voltage can be used to calculate the input power required by the electrolyser:

$$\dot{P}_{in} = IVA \quad (10)$$

The power input taken by the electrolyser is represented by $\dot{P}_{in}$, the current density is represented by I, the cell area is denoted by A and the cell voltage is V that can be determined as

$$V_{cell} = V_{conc} + V_{act} + V_{Ohm} + V_{rev} \quad (11)$$

where the first term V_{conc} denotes the concentration polarization, V_{act} represents the activation polarization, V_{Ohm} is the Ohmic polarization and V_{rev} denotes the reversible cell potential which can be evaluated for a PEM electrolyser from

$$V_{rev} = 1.229 - 85 \times 10^{-3}(T - 298) \quad (12)$$

where the cell temperature is denoted by. T.

Also, the Ohmic polarization can be evaluated for the electrolyser as

$$V_{Ohm} = RI \quad (13)$$

where R represents the cell Ohmic resistance. This resistance can be evaluated from:

$$R = dx\int_0^W \frac{1}{\zeta[\vartheta(x)]} \quad (14)$$

where the membrane ionic conductivity is denoted by ζ, the content of water as a function of location is represented by $\vartheta(x)$. The water content can be determined from the following equation:

$$\varphi(x) = \frac{(\varphi_a - \varphi_c)}{D}x + \varphi_c \quad (15)$$

Here, the water content at the anode and membrane as well as cathode and membrane are represented by ϑ_a and ϑ_c respectively. Also, D denotes the membrane thickness.

In addition to this, the activation polarization is determined from:

$$V_{act} = \sinh^{-1}\left(\frac{I}{2I_{EC,i}}\right)\left(\frac{RT}{F}\right) \quad (16)$$

Here, I is the current density and $I_{EC,i}$ represents the exchange current density at the anode or cathode respectively that is evaluated from:

$$I_{EC,i} = \exp\left(-\frac{\varepsilon_{act,i}}{RT}\right)I_i^{ref} \quad (17)$$

Here, the activation energy is represented by ε_{act}, whereas an exponential factor is represented by J_i^{ref}.

Further, the concentration polarization is evaluated as

$$V_{conc} = \frac{RT}{\beta\kappa F}\ln\left(\frac{I_L}{I_L - I}\right) \quad (18)$$

Here, the limiting current density is defined by I_L, the operating current density is denoted by I, κ represents the number electrons transferred and F denotes the Faraday's constant. Table 2 lists the design parameters utilized in the analysis and modeling of the PEM electrolyser.

Please cite this article as: Ishaq H et al., A solar and wind driven energy system for hydrogen and urea production with CO_2 capturing, International Journal of Hydrogen Energy, https://doi.org/10.1016/j.ijhydene.2020.01.208

Table 2 – Design and operating parameters of the PEM electrolyzer.

Parameter	Value
Faraday's constant	96486C/mol
Membrane thickness	100 μm
Cathode exponential factor	$4.6x10^3 A/m^2$
Anode exponential factor	$1.7x10^5 A/m^2$
φ_c	10
φ_a	14
Activation energy at cathode	18000J/mol
Activation energy at anode	76000J/mol
Temperature	80 °C

The energy efficiency of the PEM electrolyser can be evaluated as

$$\eta_{en,PEM} = \frac{\dot{N}_{H_2}\overline{LHV_{H_2}}}{\dot{P}_{in}} \tag{19}$$

where $\overline{LHV_{H_2}}$ denotes the molar lower heating value of hydrogen. Also, where the specific exergy of hydrogen is denoted by $\overline{ex_{H_2}}$, the exergy efficiency is defined as

$$\eta_{ex,PEM} = \frac{\dot{N}_{H_2}\overline{ex_{H_2}}}{\dot{P}_{in}} \tag{20}$$

Cryogenic air separation unit

The design equations for the major components employed to the cryogenic air separation unit are as follows:

Compressor B3A

$$\dot{m}_{s1}h_{s1} + \dot{W}_{in} = \dot{m}_{s2}h_{s2} \tag{21}$$
$$\dot{m}_{s1}ex_{s1} + \dot{W}_{in} = \dot{m}_{s2}ex_{s2} + \dot{E}x_d \tag{22}$$

Heat Exchanger B3B

$$\dot{m}_{s2}h_{s2} + \dot{m}_{s7}h_{s7} + \dot{m}_{s8}h_{s8} = \dot{m}_{s3}h_{s3} + \dot{m}_{s9}h_{s9} + \dot{m}_{s12}h_{s12} \tag{23}$$

$$\dot{m}_{s2}ex_{s2} + \dot{m}_{s7}ex_{s7} + \dot{m}_{s8}ex_{s8} = \dot{m}_{s3}ex_{s3} + \dot{m}_{s9}ex_{s9} + \dot{m}_{s12}ex_{s12} + \dot{E}x_d \tag{24}$$

Distillation column B3D

$$\dot{m}_{s4}h_{s4} + \dot{Q}_{RB} = \dot{m}_{s7}h_{s7} + \dot{m}_{s8}h_{s8} + \dot{Q}_{RC} \tag{25}$$

$$\dot{m}_{s4}ex_{s4} + \dot{E}x_{\dot{Q}_{in}} = \dot{m}_{s7}ex_{s7} + \dot{m}_{s8}ex_{s8} + \dot{E}x_{\dot{Q}_{in}} + \dot{E}x_d \tag{26}$$

Turbine B3F

$$\dot{m}_{s9}h_{s9} = \dot{m}_{s10}h_{s10} + \dot{W}_{out} \tag{27}$$

$$\dot{m}_{s9}ex_{s9} = \dot{m}_{s10}ex_{s10} + \dot{W}_{out} + \dot{E}x_d \tag{28}$$

Ammonia synthesis unit

In the ammonia reactor, it only needs heat to initiate the reactions and the reaction itself is exothermic. The nitrogen separated by the cryogenic air separation unit and hydrogen from PEM electrolyzer are employed to produce ammonia. The chemical and design equations are as follows:

$$N_2 + 3H_2 \rightarrow 2NH_3$$

Reactor

$$\dot{m}_{s11}h_{s11} + \dot{m}_{H_2}h_{H_2} = \dot{m}_{NH_3}h_{NH_3} + \dot{Q}_{out} \tag{29}$$

$$\dot{m}_{s11}ex_{s11} + \dot{m}_{H_2}ex_{H_2} = \dot{m}_{NH_3}ex_{NH_3} + \dot{E}x_{\dot{Q}_{out}} + \dot{E}x_d \tag{30}$$

Urea synthesis unit

In urea production, the first step which is ammonium carbamate production is exothermic while the second step for urea production is endothermic. The chemical and design equations which are employed during the system analysis are as follows:

$$2NH_3 + CO_2 \rightarrow NH_2COONH_4$$

$$NH_2COONH_4 \rightarrow (NH_2)_2CO + H_2O$$

CO_2 capture

$$\dot{m}_{NH_3}h_{NH_3} + \dot{m}_{CO_2}h_{CO_2} = \dot{m}_{carb}h_{carb} + \dot{Q}_{out} \tag{31}$$

$$\dot{m}_{NH_3}ex_{NH_3} + \dot{m}_{CO_2}ex_{CO_2} = \dot{m}_{carb}ex_{carb} + \dot{E}x_{\dot{Q}_{out}} + \dot{E}x_d \tag{32}$$

Decomposition

$$\dot{m}_{carb}h_{carb} = \dot{m}_{urea}h_{urea} + \dot{m}_{H_2O}h_{H_2O} + \dot{Q}_{out} \tag{33}$$

$$\dot{m}_{carb}ex_{carb} = \dot{m}_{urea}ex_{urea} + \dot{m}_{H_2O}ex_{H_2O} + \dot{E}x_{\dot{Q}_{out}} + \dot{E}x_d \tag{34}$$

Overall efficiencies

The performance indicator for the proposed system is defined in terms of energy and exergy efficiencies and equations are as follows:

$$\eta_{en,ov} = \frac{(\dot{W}_{wt} + \dot{W}_{PV} - \dot{W}_{CASS} - \dot{W}_{PEM} - \dot{W}_{PEM} - \dot{W}_{PEM}) + \dot{m}_{urea}LHV_{urea} + \dot{m}_{H2}LHV_{H_2}}{\dot{P}_{wt} + \dot{Q}_{solar}} \tag{35}$$

$$\eta_{ex,ov} = \frac{(\dot{W}_{wt} + \dot{W}_{PV} - \dot{W}_{CASS} - \dot{W}_{PEM} - \dot{W}_{PEM} - \dot{W}_{PEM}) + \dot{m}_{urea}ex_{urea} + \dot{m}_{H2}ex_{H_2}}{\dot{Q}_{solar}\left(1 - \frac{T_0}{T_{sun}}\right) + \dot{P}_{wt}} \tag{36}$$

Please cite this article as: Ishaq H et al., A solar and wind driven energy system for hydrogen and urea production with CO_2 capturing, International Journal of Hydrogen Energy, https://doi.org/10.1016/j.ijhydene.2020.01.208

Results and discussion

The major results for the proposed solar PV and wind powered system are presented in this section. The renewable energy sources like solar PV and wind and electrochemical components like PEM electrolyzer are modeled in EES while remaining subsystems like cryogenic are separation system, ammonia synthesis and CO_2 elimination by reacting it with ammonia and synthesizing urea are simulated in Aspen Plus. The major operating parameters of the designed system like wind speed, solar intensity and amount of CO_2 captured by NH_3 are considered in the parametric studies.

The effect of the wind speed is drawn against the power produced by wind turbines and the hydrogen production rate in Fig. 3. The significance of this study is to investigate the effect of wind speed on the major system parameters as this power production by wind turbine is linked with hydrogen production which is further linked with ammonia production in order to capture CO_2 and synthesizing urea. Thus, this factor is not only affecting the power and hydrogen production but also the ammonia production and carbon capture as well. It can be depicted that both power produced by wind turbines and hydrogen production rate have the positive effect of increment in the wind speed. The range for the wind speed is considered from 1 to 5 m/s. Initially, the power produced by the wind turbines rises with the increment in wind speed. As this power is designed to be employed to the PEM electrolyzer, thus, this increment in the power results in increasing the hydrogen production rate via PEM electrolyzer. As the wind speed increases from 1 to 5 m/s, the power produced by wind turbines increased from 0.2 to 3.3 MW and hydrogen production increases from 0 to 31.07 g/s.

Fig. 4 exhibits the effects of nitrogen and hydrogen input flowrates on the ammonia production. The range for the moles of nitrogen and hydrogen is taken as 1:3 and effect is investigated on ammonia capacity. It can be depicted from the 3D graphical representation that ammonia capacity rises with the increment in the input flowrates and these parametric studies are significant to be conducted as these can help if scale-up is desired.

Fig. 5 exhibits the effects of air flowrate in the nitrogen and oxygen separation. A cryogenic air separation unit is employed to the energy system for nitrogen supply to the ammonia synthesis reactor. The range of the input air flowrate is taken from 85 to 130 kmol/day. The two different y-axis are used to displays the scaling for nitrogen and hydrogen flowrates. Figure shows that the flowrates of nitrogen and oxygen increase with the rise in input air flowrate in the cryogenic air separation unit. It can be depicted that the input supplies can be increased easily if the designed system is required to scale-up.

The effect of fractional conversion ratio and hydrogen flowrate on ammonia production flowrates is shown in Fig. 6. The fractional conversion ratio is taken in the range of 0.2–1 and plotted on x-axis while the hydrogen input flowrate is taken in the range of 3–7 mol/s and plotted on y-axis. The z-axis is used to represent the ammonia production capacities. It can be depicted that the ammonia production capacities are highly dependent on the fractional conversion ratio of ammonia synthesis reaction and capacities can be improved significantly by increasing the fractional conversion.

The effect of the nitrogen and hydrogen flowrates on the heat duty of the ammonia production reaction is shown in Fig. 7. Ammonia synthesis is an exothermic reaction which releases heat and this parametric study is significant to investigate the amount of heat released by the ammonia

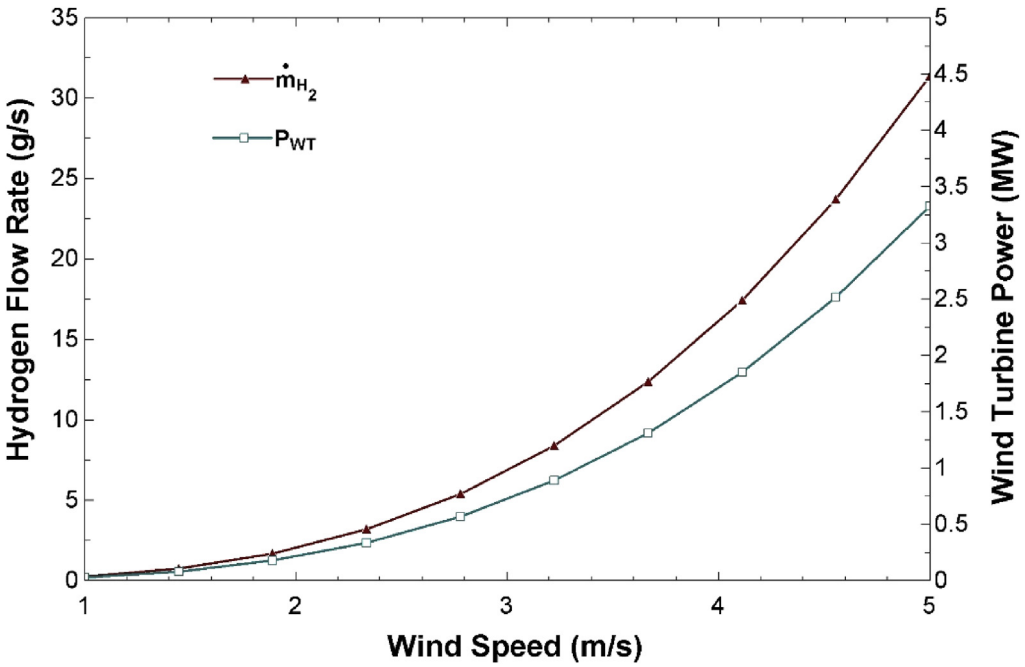

Fig. 3 – Effect of wind speed on the wind turbine power and hydrogen production rate.

Please cite this article as: Ishaq H et al., A solar and wind driven energy system for hydrogen and urea production with CO_2 capturing, International Journal of Hydrogen Energy, https://doi.org/10.1016/j.ijhydene.2020.01.208

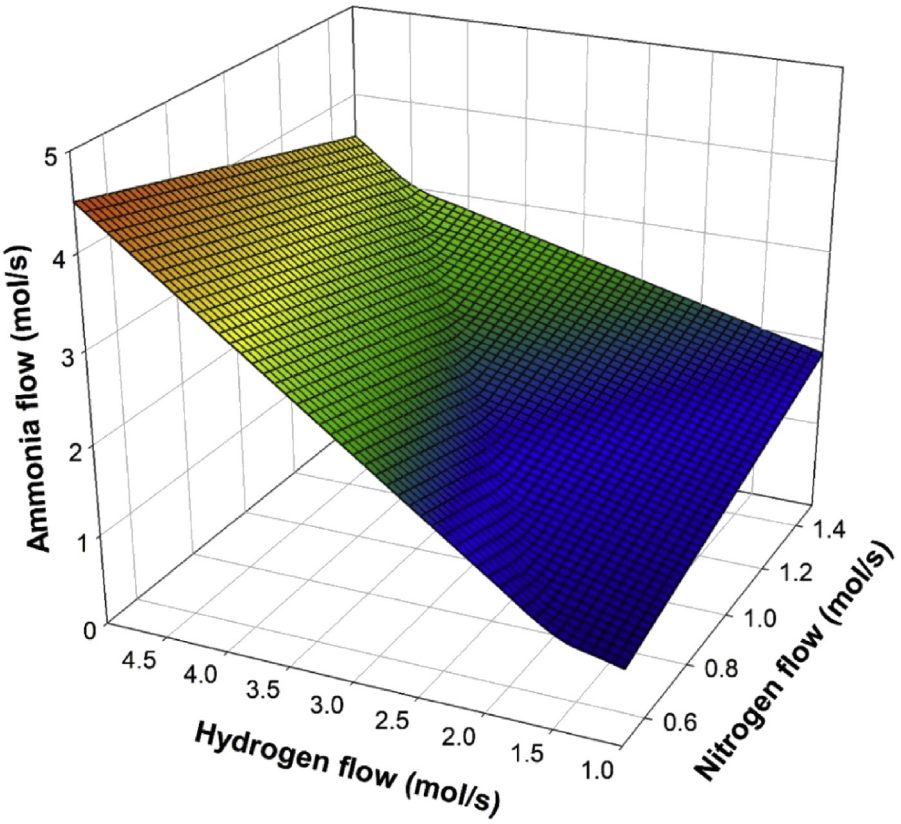

Fig. 4 – Nitrogen and hydrogen flowrates effect on the ammonia synthesis.

synthesis reaction. The flowrate of hydrogen is taken in the range of 1–5 mol/s and plotted on x-axis while the nitrogen input flowrate is taken in the range of 0.5–1.5 mol/s and plotted on y-axis. The amount of heat released by the exothermic reaction is shown by the z-axis. It can be depicted that the heat released by the ammonia synthesis reaction increases from 24.7 to 156.4 kW. Fig. 8 exhibits the effect of the amount of CO_2 which reacts with NH_3 and its effect is displayed on the ammonium carbamate flow rate as well as the urea synthesis. The significance of this study is to investigate the system potential to absorb CO_2 and also to calculate the amount of urea synthesis at different flow rates of CO_2. The Figure displays that the ammonium carbamate flow rate increases with the increment in the CO_2 amount which causes the heat duty of the reactor to increase as it is an exothermic reaction and increment in the ammonium carbamate flow rate facilitates higher urea synthesis.

The effect of the ammonium carbamate flowrate is investigated against the urea production capacity and heat absorbed by the urea synthesis reactor and study is shown in Fig. 9. As urea synthesis consists of two major steps of the ammonium carbamate production and decomposes step splits ammonium carbamate into urea. Thus, it is important to investigate the effect of ammonium carbamate flowrate on the urea production capacity and heat requirement by the urea synthesis reactions. The range for the ammonium carbamate flowrate is taken from 40 to 172.3 kmol/day. The two different Y-axis are used to displays the scaling for urea synthesis and heat absorbed by the reaction. It can be depicted that with the rise in ammonium carbamate flowrate from 40 to 172.3 kmol/day, the heat absorbed by the urea synthesis reactor increases from 11.3 kW to 46.1 kW

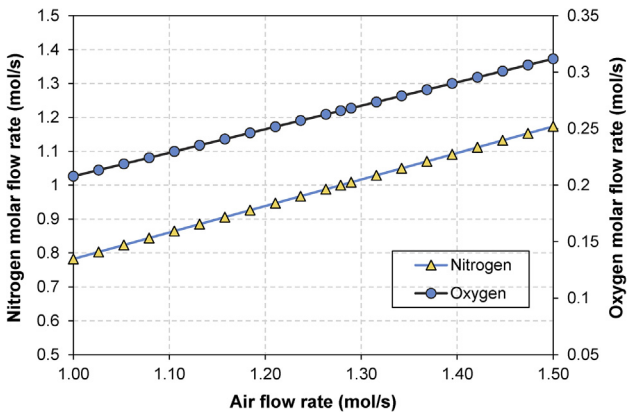

Fig. 5 – Air flowrate effect on nitrogen and oxygen separation rate.

Please cite this article as: Ishaq H et al., A solar and wind driven energy system for hydrogen and urea production with CO_2 capturing, International Journal of Hydrogen Energy, https://doi.org/10.1016/j.ijhydene.2020.01.208

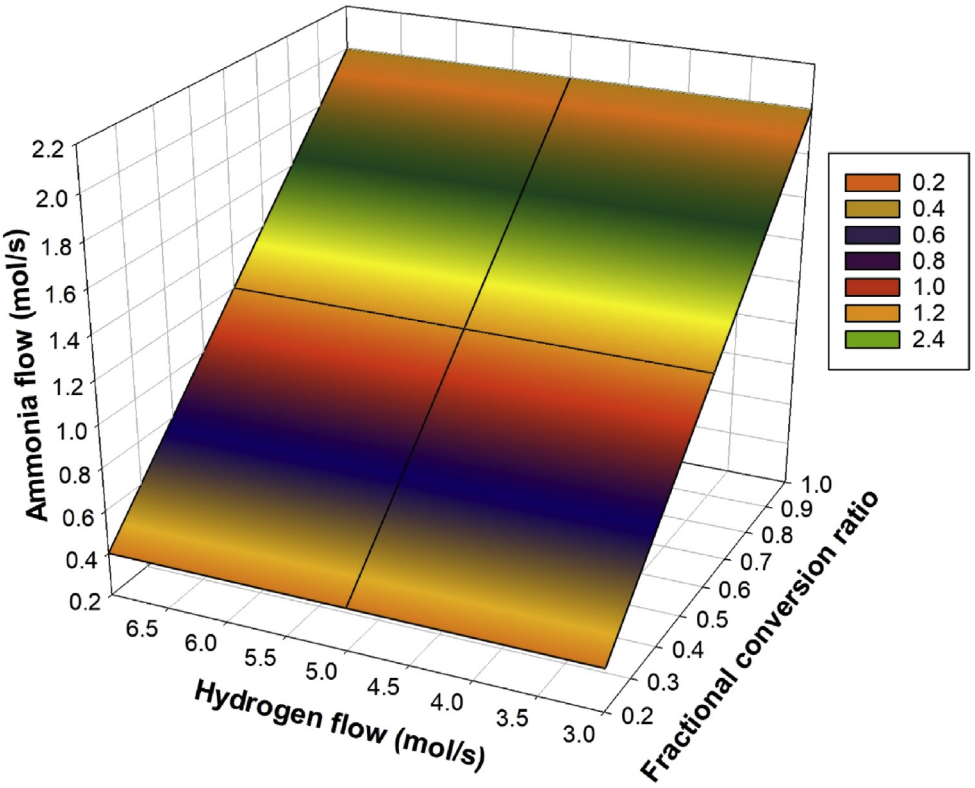

Fig. 6 – Effect of conversion ratio and hydrogen flowrate on ammonia production flowrates.

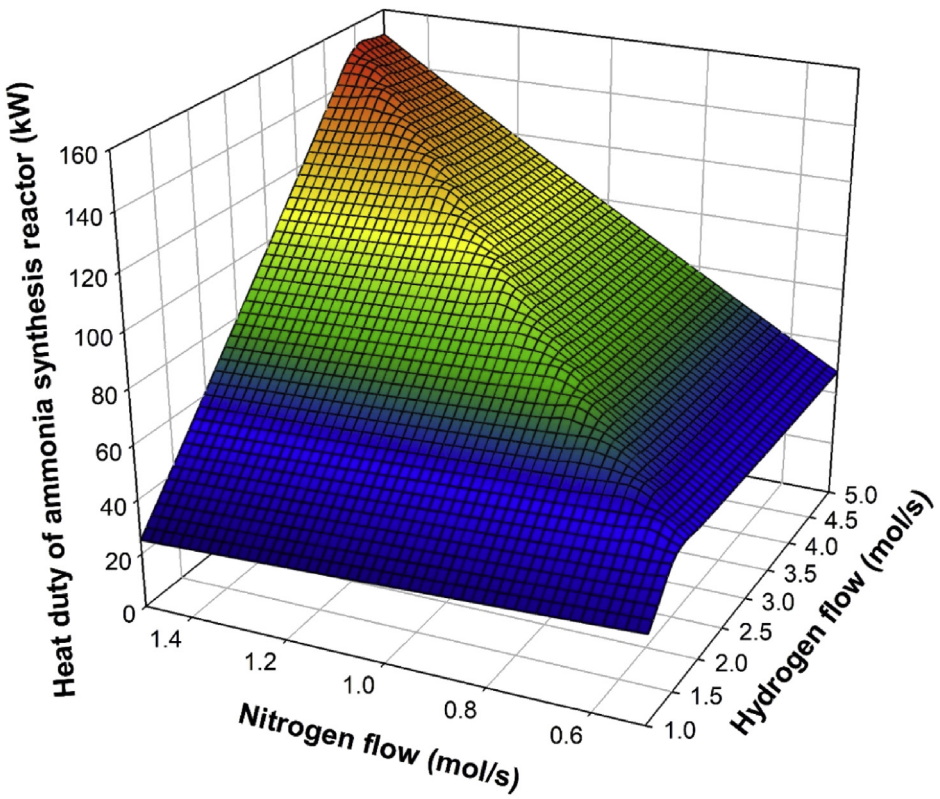

Fig. 7 – Hydrogen and nitrogen flowrates effect on the heat duty of ammonia synthesis reactor.

Please cite this article as: Ishaq H et al., A solar and wind driven energy system for hydrogen and urea production with CO_2 capturing, International Journal of Hydrogen Energy, https://doi.org/10.1016/j.ijhydene.2020.01.208

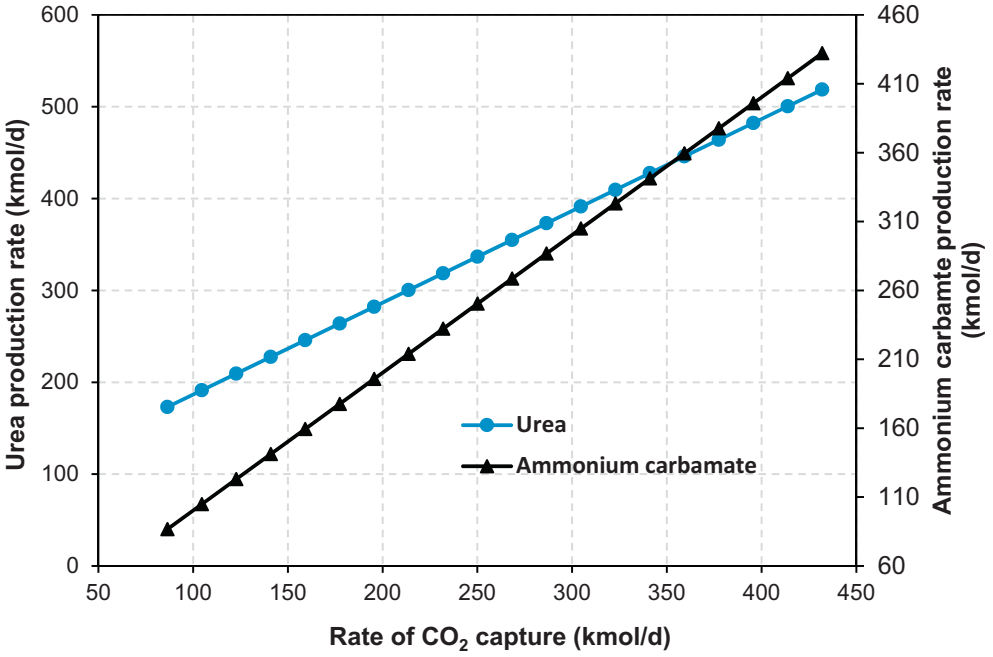

Fig. 8 – Effect of CO_2 capture on urea and ammonium carbamate production.

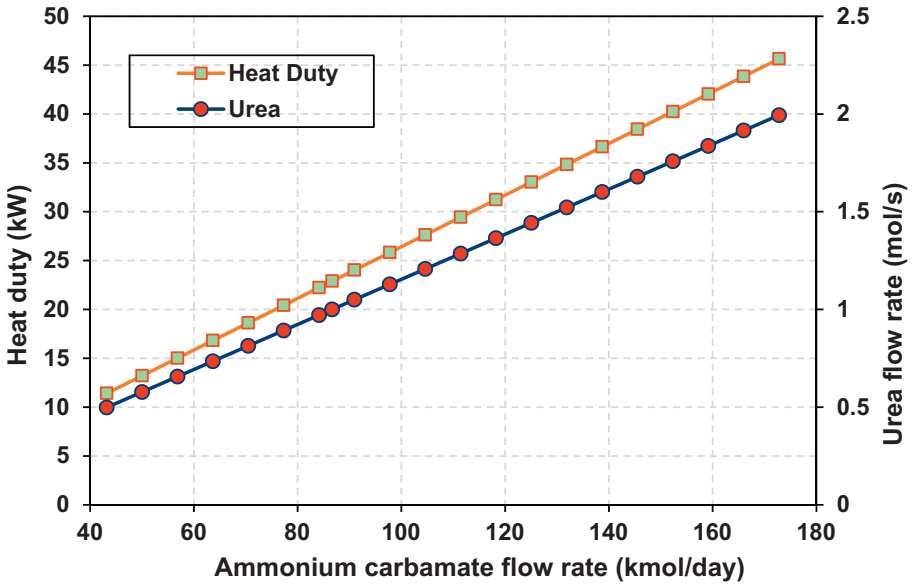

Fig. 9 – Ammonium carbamate flowrate effect on the heat duty and urea synthesis capacity.

and urea synthesis increases from 0.49 mol/s to 1.99 mol/s. The solar PV panel efficiency effect is investigated on the energetic and exergetic efficiencies of the system in Fig. 10. Table 3 represent the significant results of the proposed design such as work rates, heat rates and efficiencies. The significance of this study is to investigate the system performance under different conditions of solar PV efficiencies. The range for the efficiency is considered from 0.05 to 0.25. It can be depicted from the figure that both energy and exergy efficiencies have the positive effect of solar PV panel efficiency. As the solar PV panel efficiency rises from 0.05 to 0.25%, the overall energy efficiency increases from 22.9% and reaches to 56.6% while exergy efficiency rises from 0.17% and approaches to 41%.

Please cite this article as: Ishaq H et al., A solar and wind driven energy system for hydrogen and urea production with CO_2 capturing, International Journal of Hydrogen Energy, https://doi.org/10.1016/j.ijhydene.2020.01.208

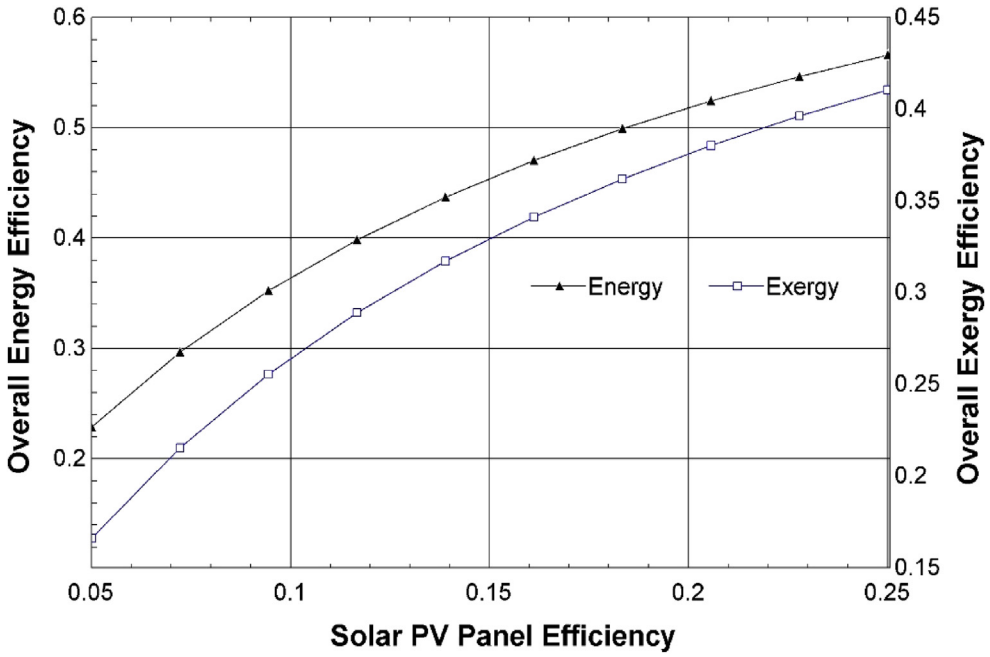

Fig. 10 – Solar PV panel efficiency effect on the energetic and exergetic efficiencies.

Table 3 – Significant results of the proposed design.

Parameter	Value	Unit
Compressor B3A work rate	13.9	kW
Compressor B3F work rate	42.4	kW
Compressor B3H work rate	299	kW
Ammonia Reactor heat rate	181.7	kW
Ammonia carbamate reactor heat rate (exothermic)	83.4	kW
Urea reactor heat rate (endothermic)	22.9	kW
Electrical power output	2.14	MW
Hydrogen production rate	518.4	kmol/d
Urea synthesis	86.4	kmol/d
Energy efficiency	44.4	%
Exergy efficiency	32.2	%

Conclusions

A solar PV and wind hybrid system is developed in this study and capturing CO_2 with ammonia and synthesizing urea is the approach considered in the system design. The major subsystems are solar PV, wind turbines, cryogenic air separation system, PEM electrolyzer, ammonia reactor and CO_2 capturing through ammonia and synthesizing urea. This approach can be employed to any industrial plant producing the CO_2 emissions. The proposed system captures industrial CO_2 emissions using renewable energy and synthesizes urea for useful purposes. The proposed design is capable of capturing 1387 tons/year of CO_2. Additionally, the electrical power, hydrogen and urea are the major commodities of the proposed design. The energetic and exergetic efficiencies of the developed system are 44.4% and 32.2% respectively.

Nomenclature

A	area (m^2)
C_p	specific heat (kJ/kg.K)
$\dot{E}n$	energy rate (kW)
F	Faraday's constant
e_x	specific exergy (kJ/kg)
FF	fill factor
h	specific enthalpy (kJ/kg)
I	current density (A/m^2)
LHV	lower heating value (kJ/kg)
$\dot{m}$	mass flow rate (kg/s)
$\dot{N}_{H_2}$	molar rate of hydrogen (mol/s)
$\dot{P}_{in}$	power input (kW)
$\dot{Q}$	specific heat (kW)
$\dot{Q}_{solar}$	solar input (kW)
R	Ohmic resistance (Ω)
s	specific entropy (kJ/kg K)
$\dot{S}_{gen}$	Entropy generation rate (kW/K)
T	temperature (°C)
V	wind speed (m/s)
V_{OC}	open circuit voltage (V)
$\dot{W}$	Power or work rate (kW)

Greek letters

η	energy efficiency
ψ	exergy efficiency
ρ_{air}	density
ζ	ionic conductivity
ϵ_{act}	activation energy
I_L	limiting current density
κ	number of electrons transferred

Please cite this article as: Ishaq H et al., A solar and wind driven energy system for hydrogen and urea production with CO_2 capturing, International Journal of Hydrogen Energy, https://doi.org/10.1016/j.ijhydene.2020.01.208

Subscripts

0	reference conditions
act	activation
Comp	compressor
conc	concentration
elect	electrolyser
i	input
ohm	Ohmic
OC	open circuit
rev	reversible
SC	short current
W	work

Acronyms

CASU	Cryogenic Air Separation Unit
HEX	Heat Exchanger
PEM	Proton Exchanger Membrane
EES	Engineering Equation Solver

REFERENCES

[1] United States Environment Protection Agency. Sources of greenhouse gas emissions greenhouse gas (GHG) emissions US EPA [cited 20 January 2020]. Available from: https://www.epa.gov/ghgemissions/sources-greenhouse-gas-emissions.

[2] Davison J, Thambimuthu K. Technologies for capture of carbon dioxide. Greenh Gas Control Technol 2005:3–13. https://doi.org/10.1016/B978-008044704-9/50002-1.

[3] Apak R. Alternative solution to global warming arising from CO2 emissions - partial neutralization of tropospheric H2CO3 with NH3. Environ Prog 2007;26:355–9.

[4] Barzagli F, Mani F, Peruzzini M. Carbon dioxide uptake as ammonia and amine carbamates and their efficient conversion into urea and 1,3-disubstituted ureas. J CO2 Util 2016. https://doi.org/10.1016/j.jcou.2015.12.006.

[5] Barzagli F, Mani F, Peruzzini M. From greenhouse gas to feedstock: formation of ammonium carbamate from CO2 and NH3 in organic solvents and its catalytic conversion into urea under mild conditions. Green Chem 2011;13:1267–74.

[6] Bandyopadhyay A. Amine versus ammonia absorption of CO_2 as a measure of reducing GHG emission: a critical analysis. Clean Technol Environ Policy 2011;13:269–94.

[7] McLarnon CR, Duncan JL. Testing of ammonia based CO_2 capture with multi-pollutant control technology. Energy Procedia 2009;1:1027–34.

[8] Kozak F, Petig A, Morris E, Rhudy R, Thimsen D. Energy procedia chilled ammonia process for CO 2 capture. Energy Procedia 2009;1:1419–26.

[9] Pérez-Calvo JF, Sutter D, Gazzani M, Mazzotti M. Application of a chilled ammonia-based process for CO2 capture to cement plants. Energy Procedia 2017;114:6197–205. Elsevier Ltd.

[10] Rhee CH, Kim JY, Han K, Ahn CK, Chun HD. Process analysis for ammonia-based CO2 capture in ironmaking industry. Energy Procedia 2011;4:1486–93. Elsevier Ltd.

[11] Gaspar J, Arshad MW, Blaker EA, Langseth B, Hansen T, Thomsen K, Von Solms N, Fosbøl PL. A low energy aqueous ammonia CO2 capture process. Energy Procedia 2014;63:614–23. Elsevier Ltd.

[12] Hydrochloric acid recovery from exhausted metal pickling baths.

[13] Puxty G, Rowland R, Attalla M. Comparison of the rate of CO2 absorption into aqueous ammonia and monoethanolamine. Chem Eng Sci 2010;65:915–22.

[14] Qin F, Wang S, Kim I, Svendsen HF, Chen C. Study of the heat of absorption of co2 in aqueous ammonia: comparison between experimental data and model predictions. Ind Eng Chem Res 2010;49:3776–84.

[15] Dave N, Do T, Puxty G, Rowland R, Feron PHM, Attalla MI. CO 2 capture by aqueous amines and aqueous ammonia-A Comparison. Energy Procedia 2009;1:949–54.

[16] Valenti G, Bonalumi D, Macchi E. Energy and exergy analyses for the carbon capture with the Chilled Ammonia Process (CAP). Energy Procedia 2009;1:1059–66.

[17] Jilvero H, Normann F, Andersson K, Johnsson F. Thermal integration and modelling of the chilled ammonia process. Energy Procedia 2011;4:1713–20. Elsevier Ltd.

[18] Kurz F, Rumpf B, Maurer G. Vapor-liquid-solid equilibria in the system NH3CO2H2O from around 310 to 470 K: New experimental data and modeling. Fluid Phase Equil 1995;104:261–75.

[19] Bennett R, Clifford S, Anderson K, Puxty G. Carbon capture powered by solar energy. Energy Procedia 2017;114:1–6. Elsevier Ltd.

[20] Li H, Yan J, Campana PE. Feasibility of integrating solar energy into a power plant with amine-based chemical absorption for CO 2 capture. Int J Greenh Gas Control 2012;9:272–80.

[21] Zhao Y, Hong H, Zhang X, Jin H. Integrating mid-temperature solar heat and post-combustion CO 2-capture in a coal-fired power plant. Sol Energy 2012;86:3196–204.

[22] Ordorica-Garcia G, Delgado AV, Garcia AF. Novel integration options of concentrating solar thermal technology with fossil-fuelled and CO2 capture processes. Energy Procedia 2011;4:809–16. Elsevier Ltd.

[23] European Fertilizer Manufacturers' Association. Production of urea and ammonium nitrate. Belgium: EFMA; 2000.

Please cite this article as: Ishaq H et al., A solar and wind driven energy system for hydrogen and urea production with CO_2 capturing, International Journal of Hydrogen Energy, https://doi.org/10.1016/j.ijhydene.2020.01.208